Correlation between Structural Relaxation and Distribution of Particle Clusters in Glass-Forming Epoxy−Amine Mixtures Undergoing Step Polymerization

R. Volponi,[†] S. Corezzi,*[,†,‡] and D. Fioretto[†,‡]

Dipartimento di Fisica, Università di Perugia, Via A. Pascoli, I-06123, Perugia, Italy, and CNR-INFM CRS-Soft, c/o Università di Roma "La Sapienza", P. A. Moro 2, I-00185 Roma, Italy

Received November 28, 2006; Revised Manuscript Received February 16, 2007

ABSTRACT: The evolution of the structural relaxation during the step polymerization process of four different formulations of an epoxy−amine mixture—diglycidyl ether of Bisphenol A with diethylenetriamine—has been studied by means of broadband dielectric spectroscopy. Step polymerization progressively turns the liquid into a glass and offers an efficient means to study the effect of the formation of clusters of bonded particles on the structural dynamics. Specifically, we investigate how changes in the distribution of particle clusters reflect in the slowdown and broadening of the relaxation process. We find that the average cluster size diverges as the system freezes at the glass transition and relates to the structural relaxation time in a manner formally similar to that predicted for the size of the cooperatively rearranging regions within the Adam−Gibbs model for glass-forming liquids. This result confirms the one previously obtained by photon correlation spectroscopy on the same systems and indicates it is independent of the experimental technique. Moreover, we observe that the low-frequency broadening of the relaxation function on approaching the glass transition is connected to the increasing polydispersity of the system. We quantify this polydispersity by the variance σ of the cluster size distribution or by the steepness a of the distribution tail, and we find, over a wide range of these parameters, that the low-frequency power-law exponent m of the relaxation function is linear vs log a and log σ.

A. Introduction

Structural arrest related to the glass transition is a topic of great interest in material science. Glasses can be formed by many routes,[1] the more traditional being reducing the temperature or increasing the pressure of a viscous fluid, fast enough to avoid crystallization. Other technologically relevant paths to glass formation include vapor deposition, concentration increase in colloidal suspensions, solvent evaporation, and liquid polymerization reactions. Finding a common paradigm for such a wide class of structural arrest phenomena is an actual challenge. In this direction, even though we are far from a comprehensive description of the dynamics of liquids from the onset of the structural relaxation to the structural arrest, cooperativity studies[2−7] in conjunction with the Adam−Gibbs entropy model[8] suggest that growing up of particle clusters may be at the core of glass formation.

Epoxy systems show a great potential to test ideas related to glass formation, as they easily form glasses via thermal or pressure paths or can be isothermally isobarically vitrified via step polymerization if cured with hardener agents like amines. Their temperature[9−15] and pressure[16−20] behavior has long been studied, using different experimental methods. A number of techniques, including calorimetry,[21−30] ultrasound[31−33] and shear measurements,[34,35] infrared,[35−39] light scattering,[30,31,36,40−42] and dielectric spectroscopy,[17,29,36,43−53] can also be used to investigate the dynamics and thermodynamics of epoxy-based systems during polymerization reaction. The comparison of results obtained by different spectroscopic techniques is of fundamental importance to distinguish features which are genuine manifestations of the glass transition from those which are related to molecular details or to the technical probe.

Epoxy-based step polymers, in particular, can serve as an excellent model for studying the clustering process and its connection with the structural arrest. Differently from the case of liquids undergoing thermal and pressure-induced vitrification, in fact, an unambiguous definition of cluster can be given for systems undergoing step polymerization, as a set of permanently bonded monomers present in the system at a certain extent of the polymerization reaction. The extent of polymerization is quantified by the epoxy conversion α, i.e., the fraction of epoxy groups reacted, which can be measured by calorimetry[21−30] or infrared spectroscopy experiments.[35−39] At any value of α, the distribution of clusters is known in many cases from well-established statistical models.[54,55] From this information a connection between structural relaxation properties near the glass transition and properties of the growing clusters can be traced. An example is provided by the relationship between increase of the average cluster size and increase of the structural relaxation time recently derived for a series of epoxy−amine formulations on the basis of results from photon correlation spectroscopy (PCS).[56] On intuitive grounds, one also expects a relationship between the shape of the cluster distribution and the shape of the structural relaxation. Within a heterogeneous picture of relaxation, in particular, a broader distribution of clusters is expected to give rise to a broader relaxation function. It should be noted, however, that despite that a mechanism of broadening related to spatial heterogeneities has been invoked by different authors,[36,57,58] it is not demonstrated experimentally stringent investigations being generally prevented by the absence of direct access to properties of these heterogeneities to be compared with measured relaxation properties on the same system.

In this paper we report new broadband dielectric spectroscopy (DS) measurements on four different formulations of an epoxy−amine mixture, undergoing step polymerization.[59] The reaction

* Corresponding author. E-mail: corezzi@fisica.unipg.it.
[†] Università di Perugia.
[‡] Università di Roma "La Sapienza".

10.1021/ma0627323 CCC: $37.00
Published on Web 03/31/2007

proceeds via random formation of covalent bonds between the amino hydrogen and epoxy group. On increasing the number of bonds in the system, the growing clusters of momomers progressively slow down, while their size becomes widely distributed and the spatial heterogeneity in the system increases. Focusing on the structural relaxation process, we analyze the changes in relaxation time and spectral shape during the polymerization reaction and study how they correlate with the attendant variation of the distribution of clusters in the system. In particular, we compare in section D1 the behavior of the relaxation time as a function of α with the corresponding variation of the average cluster size and with related predictions of the entropy model.[60] Changes in shape of the relaxation function are considered in section D2, in connection with the broadening of the cluster size distribution. By changing the molar ratio of the monomer constituents, we investigate systems characterized by different reaction kinetics, leading to different cluster size distributions, and different gelation and glass transition points. The present results are discussed in comparison with those obtained by PCS on the same systems.

B. Experimental Section

The epoxy compound diglycidyl ether of bisphenol A (DGEBA, molecular weight 348) and the curing agent diethylenetriamine (DETA, ≥99%) were used as received by Aldrich. We studied four DGEBA−DETA formulations, with the molar ratio N_e:N_a between epoxy and amino reagent equal to 10:3, 5:2, 5:2,8, and 10:9. Since DGEBA bears two epoxy functional groups and DETA five amino functional groups per molecule, our mixtures realize the condition of an excess of epoxy groups, the stoichiometric balance of functional groups, and an excess of amino groups. Each mixture was prepared by mixing for 2−3 min at room temperature and then transferred into the measurement cell, kept at a fixed temperature.

Cure reaction of DGEBA with DETA proceeds via stepwise polyaddition of the amino hydrogen to the epoxy group. Thus, a convenient measure of the extent of reaction is the epoxy conversion α, i.e., the fraction of epoxy groups that have reacted since the beginning of the reaction. To determine α, we measured via differential scanning calorimetry the heat release associated with chemical bond formation. At any reaction time t, $\alpha(t)$ was calculated by the ratio $\Delta H(t)/\Delta H_{tot}$ (per gram of mixture), where $\Delta H(t)$ is the heat released up to the time t and ΔH_{tot} is the heat release associated with the total consumption of epoxy functional groups. For more details see ref 30. From repeated measurements we estimate the accuracy of our conversion data to be 1.5%.

Because of the presence of a multifunctional reagent, the cure of DGEBA with DETA grows branched molecules and finally yields a network polymer. Before a solid glass, the system develops into a gel, which is a system able to sustain shear stress due to the presence of a network of bonded particles spanning a macroscopic portion of the sample. The extent of reaction at the gel point, according to the classical theory of Flory,[61] is $\alpha_{gel} = 0.43$, 0.50, 0.59, and 0.75 for our four mixtures.

Dielectric spectroscopy measurements were carried out in the frequency range 10^{-1}−10^6 Hz by means of an Alpha Novocontrol analyzer, employing a parallel plates measurement cell. The reaction temperature was fixed at 32, 28, 26, and 22 °C for the mixtures DGEBA−DETA 10:3, 5:2, 5:2,8, and 10:9, respectively. At these temperatures the polymerization reaction typically takes 6−7 h to reach completion. As the acquisition of each dielectric spectrum only takes 3−4 min, the advancement of reaction over a single relaxation measurement can be considered negligible, and the dielectric evolution of the system is monitored by a succession of quasi-equilibrium states, each associated with a certain value of epoxy conversion α.

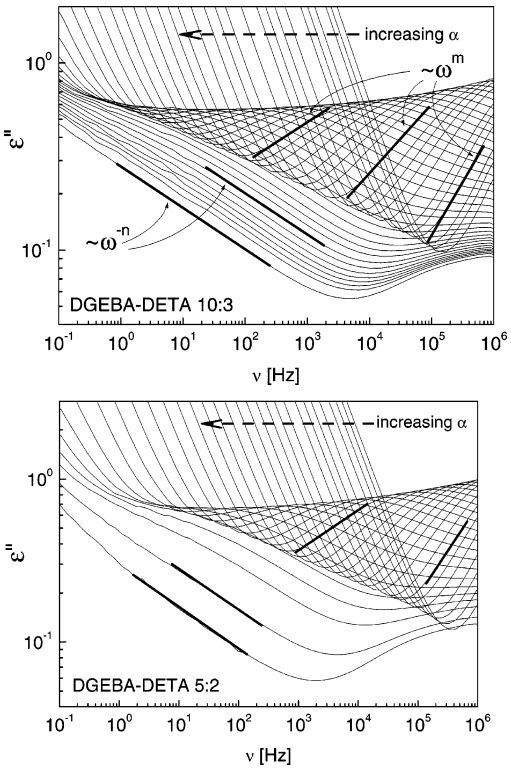

Figure 1. Dielectric loss spectra of DGEBA−DETA 10:3 and DGEBA−DETA 5:2 reactive mixtures, cured at 32 and 28 °C, respectively. In the direction of the dashed arrow, the spectra are acquired at increasing times of reaction, thus corresponding to increasing values of epoxy conversion α. Bold segments are drawn to highlight the power-law behavior of the structural relaxation function at low ($\sim\omega^m$) and high frequencies ($\sim\omega^{-n}$): a continuous decrease of m and an almost constant behavior of n are clearly seen.

C. Results

Figure 1 shows typical dielectric loss spectra ϵ'' for the reactive systems DGEBA−DETA 10:3 and DGEBA−DETA 5:2, acquired at different reaction times during cure under isothermal conditions. The evolution of the spectra strictly reflects the glass transition process that occurs as a result of the polymerization reaction. On increasing the number of bonds between monomers, i.e., α, the movements that permit the molecules to change their positions become increasingly slow; correspondingly, the structural process moves toward lower frequencies. When the characteristic time for the structural rearrangements becomes longer than the duration of a typical experiment ($\sim 10^2$ s), the system appears to be arrested and then enters the glassy state. Approximately at the same time, diffusion at a molecular level is blocked up and polymerization stops. Since the structural relaxation process dominates the spectra, its evolution can roughly be described through the frequency ν_{max} of maximum ϵ'', which is taken by visual inspection of the spectra and converted into a relaxation time $\tau^* = (2\pi\nu_{max})^{-1}$, reported in Figures 4a−7a as a function of α. Unfortunately, at least two other features in the spectra are able to perturb the detection of the structural relaxation time: a steep $\sim\omega^{-1}$ increase of ϵ'' with decreasing frequency, related to ionic conductivity, which contributes less on increasing α, and a secondary relaxation process at higher frequencies, more evident in the final stage of the reaction, when the structural relaxation has shifted to the low-frequency side of the spectral window. This complex scenario can make the frequency of maximum structural dielectric loss be different from the frequency of maximum total dielectric loss and may alter its dependence on α. To remove this effect, we separate the contribution to the spectra

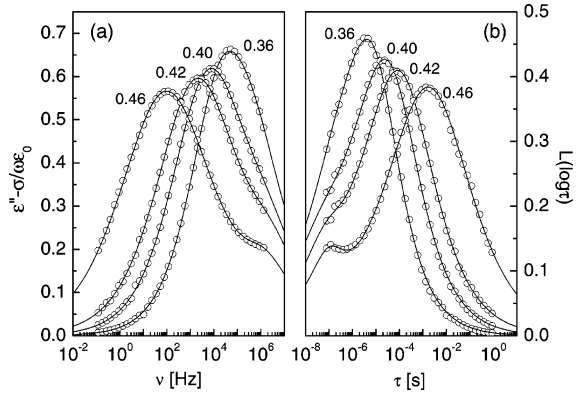

Figure 2. (a) Dielectric loss without the ionic conductivity contribution and (b) the corresponding retardation spectra for the system DGEBA−DETA 10:3 at the indicated values of conversion.

of the structural relaxation through a full-spectrum analysis performed by modeling the complex dielectric function $\epsilon^* = \epsilon' - i\epsilon''$ as the sum of a conductivity term and two Havriliak−Negami (HN) terms

$$\epsilon^*(\omega) - \epsilon_\infty = \frac{\sigma}{i\omega\epsilon_0} + \frac{\Delta}{[1 + (i\omega\tau_{HN})^a]^b} + \frac{\Delta_s}{[1 + (i\omega\tau_s)^{a_s}]^{b_s}} \quad (1)$$

where $\omega = 2\pi\nu$ is the angular frequency, ϵ_∞ is the high-frequency limit of $\epsilon'(\omega)$, ϵ_0 is the vacuum permittivity, σ is the dc conductivity, Δ, τ_{HN}, a, and b are the amplitude, characteristic time, and shape parameters of the structural relaxation process, and the parameters with index s refer to the secondary relaxation. The use of the phenomenological HN function to model the relaxation processes is motivated by the direct evidence in ϵ'' (see Figure 1) of power law behaviors for the high ($\sim\omega^{-n}$) and low-frequency limit ($\sim\omega^m$) of the structural relaxation and for the low-frequency limit of the secondary process. The HN function properly describes these power law behaviors, with $m = a$ and $n = ab$.

To test the robustness of our fit results, the dielectric loss curves $\epsilon''(\omega)$ are also converted into retardation time spectra $L(\ln\tau)$ and analyzed according to the procedure explained in refs 65 and 66. Retardation spectra calculated for the system DGEBA−DETA 10:3 at different values of conversion are shown in Figure 2, together with the corresponding dipolar relaxation spectra obtained by subtracting the conductivity contribution to the dielectric loss. Deconvolution of the structural and secondary contributions is carried out by describing the retardation spectrum as the sum of two terms, each corresponding to a HN function in the frequency domain[65,66]

$$L_{HN}(\ln\tau) = \frac{\Delta}{\pi}\frac{(\tau/\tau_{HN})^{ab}\sin(b\theta)}{[(\tau/\tau_{HN})^{2a} + 2(\tau/\tau_{HN})^a\cos(\pi a) + 1]^{b/2}} \quad (2)$$

where the parameter θ can be written as $\theta = \arctan x + (1 - x/|x|)\pi/2$, with $x = \sin(\pi a)/[(\tau/\tau_{HN})^a + \cos(\pi a)]$. As an example, the overall retardation spectrum and the deconvoluted structural and secondary contributions are shown in Figure 3 for the system DGEBA−DETA 10:3 at conversion $\alpha = 0.42$. The parameters obtained from the fit of the retardation spectra using eq 2 always agree within the error with those obtained from the fit of $\epsilon''(\omega)$ using eq 1.[62] The quality of the fit is quite comparable as the relative errors plotted in the insets of Figure 3 demonstrate.

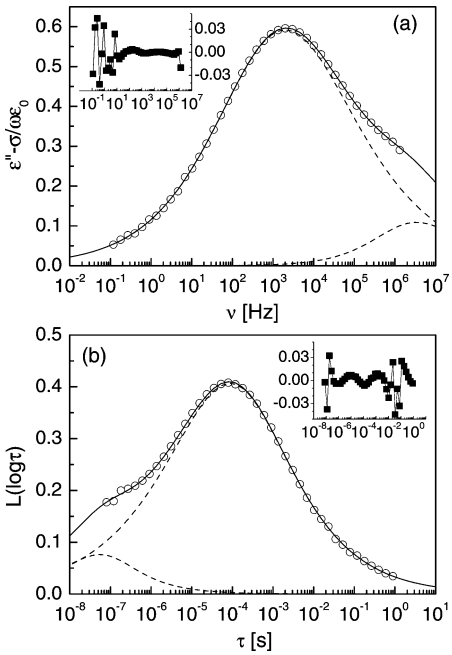

Figure 3. (a) Dielectric loss without the ionic conductivity contribution, for the system DGEBA−DETA 10:3 at conversion $\alpha = 0.42$. The circles and the solid line represent respectively the experimental data and the fit with eq 1. Dashed lines indicate the contributions of the structural and secondary relaxations. (b) Deconvolution of the calculated retardation spectrum (circles) for the system DGEBA−DETA 10:3 at conversion $\alpha = 0.42$ into contributions from the structural and secondary relaxations (dash lines). In the insets, the relative error is shown.

The presence of secondary relaxations and their interrelation with the structural one in both neat and polymerizing epoxy systems has recently been studied by Beiner et al.,[63] and information on secondary relaxations in glassy DGEBA−DETA networks can be found in ref 64. In this work, as the secondary relaxation at any time of reaction results to be partially out of the spectral window investigated, we focus on the evolution of the structural relaxation only. The structural parameters obtained from a least-squares fit of eq 1 to the experimental data are reported in Figures 4−7, together with the relaxation time τ_{max} calculated from the reciprocal frequency of maximum structural dielectric loss. It can be seen that τ_{max} coincides with τ^* at high conversion values, while it progressively departs in the low conversion region due to the influence of the secondary relaxation. Moreover, a comparison of $\tau_{max}(\alpha)$ and $\tau_{HN}(\alpha)$ shows that the two are not parallel, since the shape of the relaxation function is changing during the polymerization reaction, as discussed in the next section.

A fit with eq 1 allows us to analyze the high- and low-frequency shape of the structural relaxation separately. Panels b of Figures 4−7 show that n does not change appreciably in a relatively wide region of α. Correspondingly, m markedly decreases and then levels off. This behavior can also be directly observed in Figure 1. The same figure indicates that a decrease of m affects the spectra from the beginning of the polymerization reaction. To trace the value of m back to the early stage of reaction, we have interpolated, for low values of α, the dielectric loss spectra around the minimum between the conductivity and the structural relaxation with only the conductivity term and a HN function with fixed n and Δ. From this, we have estimated the m values shown in panels b with half-open symbols, whose behavior continues that of the points obtained from the full-spectrum fit.

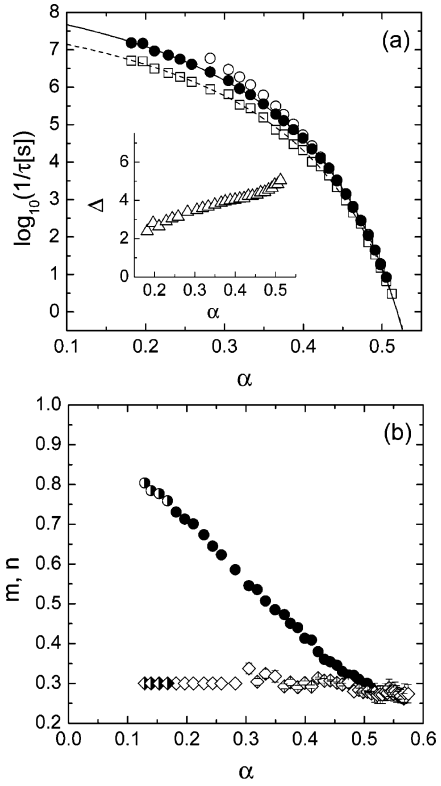

Figure 4. (a) Dependence on α of the structural relaxation time during reaction of the DGEBA−DETA 10:3 mixture. Open circles refer to τ^* evaluated from the reciprocal frequency of maximum *total* dielectric loss, open squares are τ_{HN} values obtained from a fit using eq 1, and closed cicles refer to τ_{max} evaluated from the reciprocal frequency of maximum *structural* dielectric loss. Solid and dashed lines are the best fit using eq 3. The inset shows the α dependence of the dielectric amplitude △. (b) Dependence on α of the low- and high-frequency shape parameters, *m* (circles) and *n* (diamonds), of the structural relaxation process. The value of *n* for $0.12 < \alpha < 0.28$ was kept fixed in the fit. Closed and open symbols indicate data from a full-spectrum fit using eq 1, and half-open symbols indicate data from a simplified fit procedure as explained in the text.

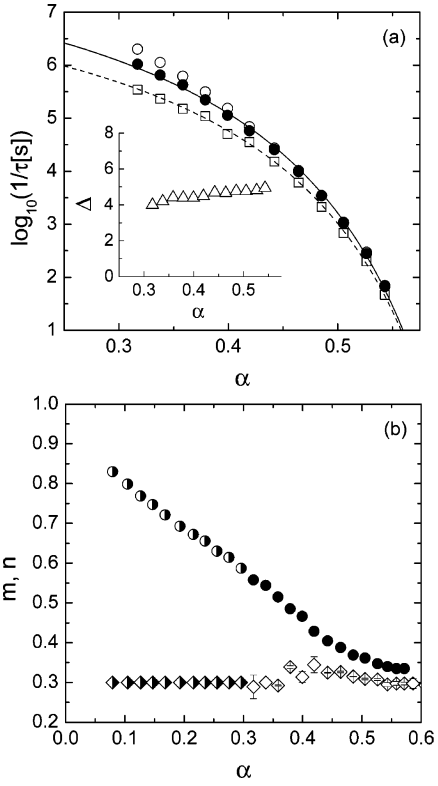

Figure 5. Same quantities as explained in Figure 4, for the DGEBA−DETA 5:2 reaction. The value of *n* for $0.08 < \alpha < 0.30$ was kept fixed in the fit.

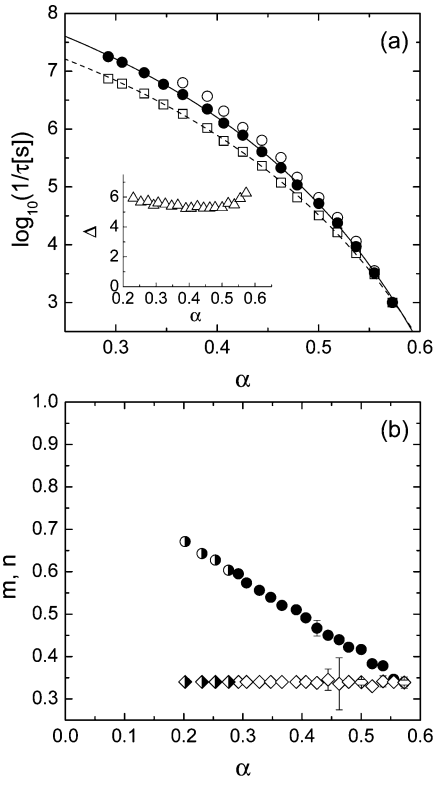

Figure 6. Same quantities as explained in Figure 4, for the DGEBA−DETA 10:9 reaction. The value of *n* for $0.20 < \alpha < 0.40$ was kept fixed in the fit.

D. Discussion

1. Relaxation Time. A qualitative inspection of the variation with α of the relaxation time of the four samples investigated shows the signature of incipient structural arrest of the systems, i.e., a rapidly increasing and apparently diverging relaxation time at sufficiently high conversions. The finally arrested material is a glassy solid. Some of our measurements extend across the gel point, but there is no observable event associated with the gelation process. Indeed, dielectric spectroscopy is blind to gelation.

The progressive slowdown of the dynamics manifests in a strongly nonlinear behavior of log τ vs α, which closely resembles the classical behavior of log τ in supercooled and overcompressed liquids, well described by Vogel−Fulcher−Tamman like (VFT) equations as a function of temperature[12,13,68] and pressure.[16,19,67] Analogously, we find the $\tau(\alpha)$ data (with $\tau \equiv \tau_{max}$ or τ_{HN}) well represented by $\tau = \tau_0 \exp[D/(\alpha_0 - \alpha)]$, with τ_0, D, and α_0 constant parameters dependent on the polymerization reaction. In particular, the conversion α_0 of apparent divergence of τ moves to higher values for increasing values of the molar ratio N_a/N_e between the amino and epoxy components. Previous workers have successfully interpreted their data for thermosetting materials (in particular, epoxy resins) in terms of an empirical law equivalent to that of the present analysis.[35,50,51] Others have questioned such law[24,26] and proposed a nonsingular three-parameter relationship between τ and α of the form $\tau = \tau_0 \exp(S\alpha^p)$, with τ_0, S, and p polymerization-dependent constants. Moving from a mere phenomenological approach, we now assess the merits of the fit with a VFT equation by examining its ability to describe the physics underlying the process.

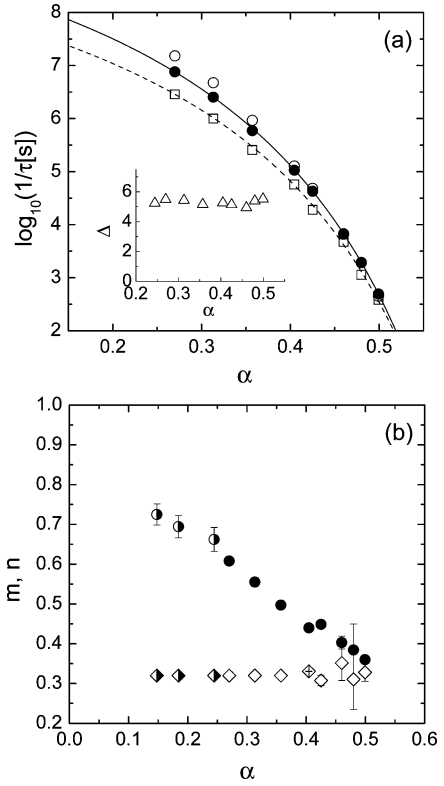

Figure 7. Same quantities as explained in Figure 4, for the DGEBA−DETA 5:2,8 reaction. The value of n for $0.15 < \alpha < 0.35$ was kept fixed in the fit.

Within an extended picture[60] of the Adam−Gibbs theory[8] of vitrification, the increase of τ during step polymerization can be explained in terms of configurational entropy changes that follow from chemical bond formation. Step polymerization produces growing covalently bonded particle clusters in the sample, whose average size x_n is predicted to vary with α as $x_n(\alpha) = 1/(1 - \bar{f}\alpha)$.[59,61] Here, $\bar{f}$ is the average epoxy functionality of the system, i.e., the average number of epoxy groups per monomer initially present in the mixture—in our case, $\bar{f} = 2N_e/(N_e + N_a)$. The clusters formed during the reaction are not big on average, x_n being of the order of 3−5 in the whole range investigated. Thus, it is reasonable that during a structural rearrangement a monomer takes the other bonded monomers along, so that all monomers in a cluster are involved in a cooperative motion. Accordingly, the size of the cooperatively rearranging regions[8] in the system increases proportionally to x_n, or equivalently, the configurational entropy S_c reduces as $S_c(\alpha) \propto 1/x_n(\alpha)$, with a consequent increase of the structural relaxation time according to $\tau = \tau_0 \exp(C/TS_c)$, with τ_0 and C constant. Hence, the relationship between τ and α reads

$$\tau(\alpha) = \tau_0 \exp(Bx_n) = \tau_0 \exp\left(\frac{B}{1 - \bar{f}\alpha}\right) \qquad (3)$$

with τ_0 constant and B only dependent on T. Notice that a VFT form now emerges within a physical picture of the glass transition process. According to eq 3, the $\tau(\alpha)$ data should appear to diverge for α approaching $1/\bar{f} = (1 + N_a/N_e)/2$, therefore, when x_n diverges. For each reaction, we fitted the data of τ_{max} for the structural relaxation with eq 3, using $1/\bar{f} = \alpha_0$, B, and τ_0 as adjustable parameters. The fit curves are drawn with solid lines in Figures 4a−7a, and the corresponding values of the parameters are listed in Table 1. The agreement between the values of α_0 obtained from the fit and the values $1/\bar{f}$ calculated from the molar ratio of the monomer constituents is very good. Equation 3 also fits the data of τ_{HN} with values of α_0 very close to those expected. This indicates that the result is robust with respect to the definition of the relaxation time chosen to describe the structural dynamics of the system. These findings constitute a positive test of the entropy theory for the structural arrest of model systems undergoing step polymerization, and state a connection between the relaxation time and an average property of the distribution of particle clusters in the system. A similar test was recently performed on the same reactive systems by means of depolarized PCS,[56] probing optical anisotropy fluctuations, which arrest at the glass transition. Also in that case a very good agreement between α_0 and calculated values of $1/\bar{f}$ was found. One of the main results of the present work is that this agreement is independent of the experimental technique used to probe the structural arrest of the system.

2. Shape Parameters. The evolution of the shape parameters in the course of reaction and the comparison with values obtained from different spectroscopic techniques deserves a separate and careful discussion. Different techniques, in fact, like DS and PCS, are sensitive to the motion of different parts of a molecule: the former to the motion of permanent electric dipoles (e.g., epoxy groups) and the latter to the motion of optically anisotropic parts (e.g., phenyl rings). Moreover, dielectric spectra are taken in the frequency domain while photon correlation spectra in the time domain, so that a Fourier transform is required before a comparison of the spectral shape. Nevertheless, one expects the shape of the structural relaxation function to be connected with features of the cooperative motions which are the same even if revealed through different physical observables.

In the epoxy−amine systems investigated, the dielectric spectra exhibit an almost constant behavior during polymerization of the high-frequency shape paramenter n and an impressive decrease of the low-frequency parameter m. In the same sytems, PCS measurements performed in the time domain give a Kohlrausch−Williams−Watt stretching parameter β_K almost constant, i.e., a time−conversion superposition of the correlation functions.[30,56] These findings are mutually consistent indeed due to the different sensitivity of the two techniques to the high- and low-frequency parts of the relaxation function. While DS ensures a good sensitivity to both parts, the shape of PCS spectra is mainly determined by the short time (high frequency) portion of the relaxation function. An unusual sensitivity of at least 3 decades in amplitude of the PCS signal is required to distinguish between single-power-law and double-power-law response.[69] Most PCS measurements have a good statistics in the short-time limit only, and so the stretching parameter β_K is the only information on the shape that can be extracted from the spectra.[70]

A further confirmation of the fact that a constant value of β_K can approximately interpolate spectra with a constant n and varying m comes from the results of a different approach commonly used to facilitate a comparison of DS with PCS spectra, consisting of fitting the dielectric spectra with the Fourier transform of the KWW function. Such an approach was used by Fitz et al.[36] in a previous investigation of a mixture DGEBA−DETA 5:2 (using DGEBA with $M_n = 374$) isothermally cured at 50 °C. A value $\beta_K = 0.28 \pm 0.02$ was found, almost constant in the conversion range $0.32 < \alpha < 0.56$, in perfect agreement with PCS results.[36,56] It should be noted, however, that this procedure allows to describe the shape of the dielectric spectra by means of a single parameter in a narrow region around the maximum of ϵ'', but it remains largely

Table 1. Best-Fit Parameters Obtained by Using Eq 3[a]

system	log τ_0 [s]	B	α_0	α_0^*	$1/\bar{f}$
DGEBA−DETA 10:3	−10.41 ± 0.06	5.37 ± 0.09	0.67 ± 0.02	0.66 ± 0.02	0.65
DGEBA−DETA 5:2	−9.2 ± 0.3	4.3 ± 0.7	0.72 ± 0.02	0.72 ± 0.02	0.70
DGEBA−DETA 10:9	−12.5 ± 0.2	8.1 ± 0.3	0.92 ± 0.02	0.94 ± 0.02	0.95
DGEBA−DETA 5:2,8	−12.1 ± 0.3	7.9 ± 0.6	0.79 ± 0.02	0.78 ± 0.02	0.78

[a] τ_0, B, and α_0 are obtained from the fit of τ_{max}; α_0^* is obtained from the fit of τ_{HN}. The last column gives $1/\bar{f} = (1 + N_a/N_e)/2$ calculated from the molar ratio of the reagents.

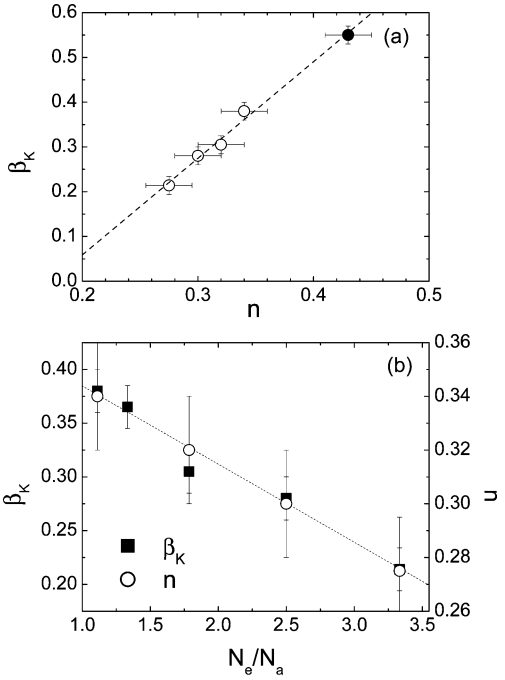

Figure 8. High-frequency HN shape parameter n for different mixtures DGEBA−DETA N_e:N_a and KWW stretching parameter β_K obtained for the same systems by PCS. The solid circle in (a) refers to neat DGEBA.

insensitive to the low-frequency shape of the dielectric function.[71]

Figure 8a compares the values of the high-frequency shape parameter n and the stretching parameter β_K in different mixtures DGEBA−DETA N_e:N_a, including the limit case of neat DGEBA, and shows that these parameters are directly related. In the mixtures they both depend on the molar ratio N_e:N_a, the relaxation function being more stretched the higher the fraction of epoxy reagent (Figure 8b). However, neat DGEBA ($n = 0.43 \pm 0.02$, $\beta_K = 0.55 \pm 0.02$)[15] does not conform to this plot, suggesting a role of local inhomogeneities in the broadening of the high-frequency side of the relaxation function.

We now concentrate on the behavior of m, whose marked decrease on increasing α, common to all the reactions investigated here, was previously observed in different epoxy-based curing systems.[17,47] The origin of this behavior has not yet been established definitely. A qualitative interpretation could be given in terms of models that relate a departure from 1 of m and n to long and short-range correlation of molecular motions, respectively controlled by inter- and intramolecular interactions.[72−76] In support of these models, a correlation between the value of m and interparticle interactions has indeed been reported for many high-molecular-weight polymers.[76] A change from $m = 1$ to $m < 1$ when passing from a monoepoxide to a diepoxide system has also been verified,[69] and broader dielectric relaxation functions have been found on increasing cross-link density in poly(vinylethylene).[58] On the other hand, there is indication that increase of long-range correlations may be not sufficient to fully explain the low-frequency broadening of the relaxation function close to the glass transition. Indication comes from the observation that broadening may be associated with a steeper cooperativity plot, i.e., with a higher apparent activation energy close to the glass transition,[58] but also be associated with the opposite effect of a reduction of apparent activation energy near T_g.[47,53]

To interpret the behavior of m, we here consider the role of spatial heterogeneities, which we have shown in the previous section to have a control role in the slowdown of the dynamics. In particular, we demonstrate in the following that the decrease of m may have a heterogeneous nature connected to the molecular polydispersity that develops during the polymerization process.

To quantify this polydispersity, we calculate first the distribution of molecular species in the system at any extent of reaction from the theory of Stockmayer for nonlinear step polymers.[54] To this purpose, we specialize the general formula to the case of a two-component mixture, consisting of N_e moles of monomers bearing f_e epoxy functional groups, together with N_a moles of monomers bearing f_a amino functional groups. When the system has polymerized until a fraction α_e of the epoxy groups and a fraction α_a of the amino groups have reacted, it has become partitioned into clusters of bonded monomers having different sizes. The number $N(x)$ of moles of molecular species consisting of x monomers (divided into x_e epoxy monomers and x_a amino monomers) is given by[54]

$$N(x) = K \sum_{\substack{x_e,x_a\geq 0 \\ x_e+x_a=x \\ f_e x_e+1\geq x \\ f_a x_a+1\geq x}} \frac{(f_e x_e - x_e)!(f_a x_a - x_a)!}{(f_e x_e - x_e - x_a + 1)!(f_a x_a - x_a - x_e + 1)!} \frac{Y^{x_e}}{x_e!} \frac{Z^{x_a}}{x_a!} \tag{4}$$

where

$$Y = \alpha_a(1 - \alpha_e)^{f_e - 1}/(1 - \alpha_a)$$

$$Z = \alpha_e(1 - \alpha_a)^{f_a - 1}/(1 - \alpha_e)$$

$$K = f_e N_e(1 - \alpha_e)(1 - \alpha_a)/\alpha_a$$

It is important to stress that the theory basic assumptions of equal reactivity of all functional groups of a given kind and no occurrence of ring formation in molecular species of finite size are reasonably verified in DGEBA−DETA mixtures. Also, note that because the addition of epoxy with amino groups is the only type of reaction, the conversion α_e of epoxy groups and the conversion α_a of amino groups are related to each other via $\alpha_a = \alpha_e f_e N_e/(f_a N_a)$, so the expression in eq 4 can be calculated as a function of the epoxy conversion only, previously and hereafter denoted in this article with α. The total number N of moles of clusters in the system is given by the sum $N = \sum_{x=1}^{x_{max}} N(x)$, where the size x_{max} of the largest possible cluster is defined by the condition $\sum_{x=1}^{x_{max}} xN(x) = N_e + N_a$. The normal-

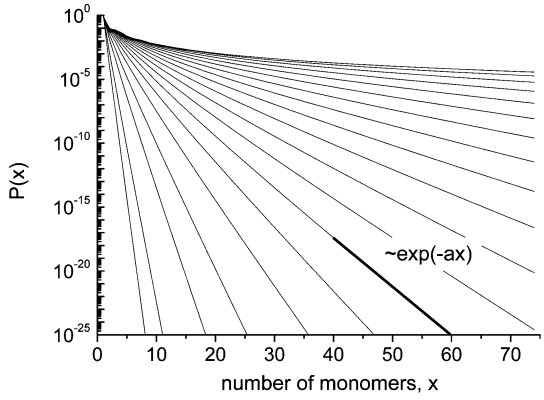

Figure 9. Normalized cluster size distribution $P(x) = N(x)/N$ for the system DGEBA−DETA 10:3, calculated from eq 4. The different curves, from left to right, correspond to increasing values of epoxy conversion α, from 10^{-4} to 0.4. On increasing α from 0, the average cluster size x_n starts to depart from 1, and a progressively higher fraction of clusters can be found with a size far from x_n (the variance, σ, of the distribution increases), distributed according to a progressively less steep probability tail (the steepness, a, decreases).

ized distribution $P(x) = N(x)/N$ represents the probability of finding a cluster with size x. As an illustration, the distribution $P(x)$ for the system DGEBA−DETA 10:3 ($f_e = 2$, $f_a = 5$) is plotted in Figure 9, with the epoxy conversion α as a parameter for the different curves. At fixed α, the molecules in the system are distributed with an average size x_n. Stoichiometric considerations lead to the formula $x_n = 1/(1 - \bar{f}\alpha)$, already mentioned in section D1. The same result is numerically obtained according to $x_n = \sum_x xP(x)$, which affords a check on the distribution formula in eq 4. The dispersion in size around the average value x_n is quantified by the variance σ of the probability distribution, defined by $\sigma^2 = \sum_x (x - x_n)^2 P(x)$.

We now demonstrate that characteristics do exist of $P(x)$ which are strictly related to each other and to the low-frequency power law exponent m of the HN function. For a fixed α, $P(x)$ is a monotonically decreasing function tending to the simple form of a power law limited by an exponential cutoff, i.e., $P(x) \sim x^{-5/2} \exp(-ax)$ for large x, as in percolation theory.[77] The parameter a represents the reciprocal of a cutoff cluster size; it will be denoted hereafter as the steepness of the distribution as it defines, in a logarithmic plot, the slope of the exponential tail of $P(x)$, as illustrated in Figure 9. Instead, the variance σ of $P(x)$ measures the spread of molecular sizes when a fraction α of the chemical bonds has formed. The advancement of reaction systematically flattens and broadens the molecular distribution; hence, the steepness decreases and the variance increases with increasing α, in a strictly correlated manner intrinsic to $P(x)$. Figure 10a,b displays the behavior of a and σ for the mixtures DGEBA−DETA investigated. (Data which fall out of the α range of our dielectric measurement have been excluded.) Figure 10c points out that in the range that concerns this study the analytic correlation between these two features of the molecular size distribution is well represented by a power law. Qualitatively, a comparison of Figure 10a and Figure 11 shows that the behavior of the steepness data closely resembles that of $m(\alpha)$. Quantitatively, a semilogarithmic plot of m vs a (Figure 12a) indeed reveals a linear behavior and therefore a logarithmic increase of the HN shape parameter m with the steepness parameter a. As flattening and broadening of $P(x)$ correlate, reduction in the exponent m and increase of σ will also result to be associated via a logarithmic relationship, as shown in Figure 12b. It should be noted that the comparison with experimental data extends over a considerable range of variation of m, although it is restricted to the pregel region since calculations using eq 4 may be affected by error close and after the gel point.

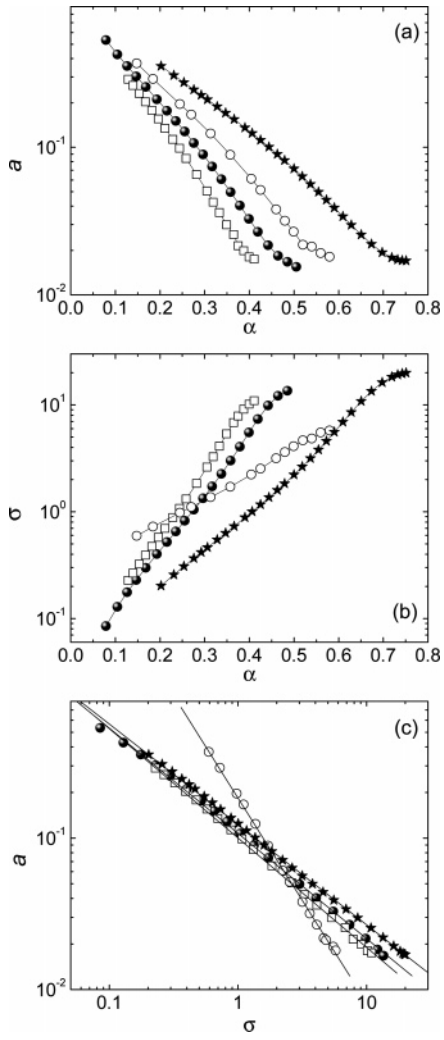

Figure 10. Variation during reaction of the parameters that characterize the normalized cluster size distribution $P(x) = N(x)/N$: (a) dependence on α of the steepness, a; (b) dependence on α of the variance, σ; (c) a vs σ on a bilogarithmic plot and the best fit (solid lines) to a power law. Data are for the mixtures DGEBA−DETA 10:3 (□), DGEBA−DETA 5:2 (●), DGEBA−DETA 5:2.8 (○), DGEBA−DETA 10:9 (★).

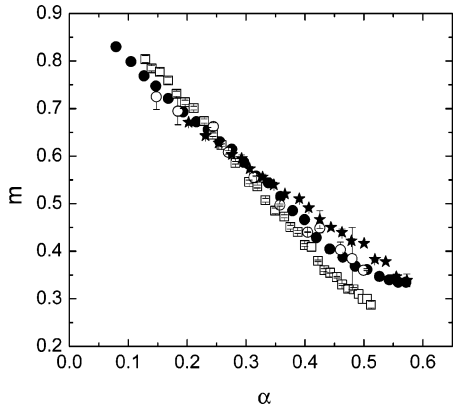

Figure 11. Dependence on α of the low-frequency HN shape parameter m for the mixtures DGEBA−DETA 10:3 (□), DGEBA−DETA 5:2 (●), DGEBA−DETA 5:2.8 (○), and DGEBA−DETA 10:9 (★).

We stress that Figure 12 demonstrates the existence of a strict correlation between the decrease of m and the development of molecular polydispersity in the system. In particular, a loga-

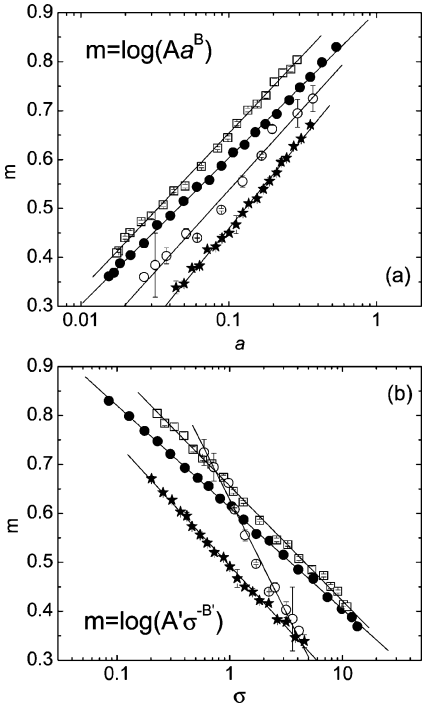

Figure 12. Variation during reaction of the HN shape parameter *m* vs (a) the steepness *a* and vs (b) the variance σ of the normalized cluster size distribution. Solid lines are best fits to a logarithmic law. Symbols are as in Figure 10.

rithmic dependence of *m* on σ (and *a*) is inferred. On the other hand, the almost constant behavior of *n* as a function of α indicates that the high-frequency tail of the relaxation function is marginally affected by polydispersity.

It is now interesting to note that our results also establish a nontrivial link between molecular polydispersity and broadening of the dielectric function, a quantity frequenly discussed in the literature in connection with the glass transition. More specifically, it is possible to show that the present results can be turned into a relationship between the variance σ and the dielectric broadening toward low frequencies W_{lf}, which is the broadening most controlled by the shape parameter *m*. We quantify W_{lf} through the width at half-height (in decades) of $\epsilon''(\omega)$, measured from the peak frequency to the lowest frequency. In order to identify how W_{lf} and σ relate to each other, we first determine how W_{lf} depends on the shape of the HN function. We chart in Figure 13 the results for this property of the HN function, by reporting *m* vs W_{lf} for fixed values of *n*. In the range of *m* and *n* which is relevant to the present paper the data for each *n* are described by a power law (straight lines), with exponent ranging from -1.10 for $n = 0.2$ to -0.92 for $n = 0.5$. In particular, the points corresponding to the pairs (*m*,*n*) measured in the course of the reactions DGEBA−DETA here investigated are represented by $m \sim W_{lf}^{-1.04\pm0.01}$. This means that in the present case an inverse proportionality well approximates our natural understanding that the lower *m*, the broader the low-frequency dielectric loss. Using $m \sim W_{lf}^{-1.04}$ allows us to put the data in Figure 12b in a manner that a quantitative link becomes apparent for all DGEBA−DETA mixtures between the broadening σ of the cluster size distribution and the low-frequency broadening W_{lf} of the dielectric response (Figure 14).

The nontrivial observation of a quantitative link between the low-frequency shape of the relaxation function and parameters that characterize the molecular polydispersity is confirmed by the analysis of literature data for other epoxy-based reactions.[17,47] The results are summarized in Figures 15−17. The data

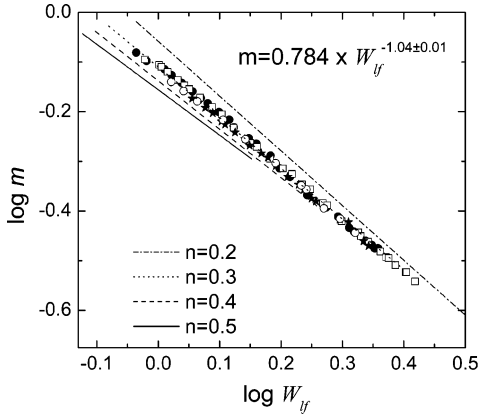

Figure 13. HN shape parameter *m* vs the low-frequency width of $\epsilon''(\omega)$, W_{lf}. For fixed values of *n*, the data follow straight lines. Symbols (the same as in Figure 10) mark points corresponding to measured pairs (*m*, *n*) in the course of the reactions DGEBA−DETA investigated; overall, they are represented by the indicated power law.

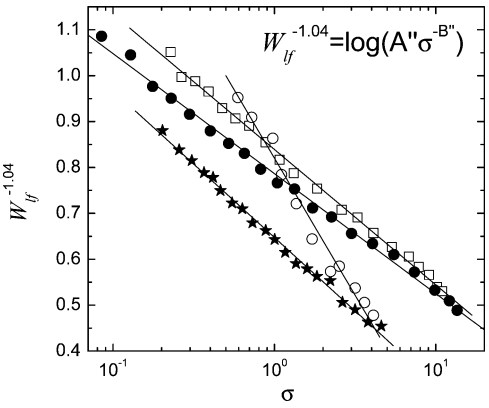

Figure 14. Variation during reaction of the low-frequency width of $\epsilon''(\omega)$, W_{lf}, vs the corresponding broadening of the cluster size distribution, σ. Symbols are as in Figure 10. Straight lines are best fits to a logarithmic law.

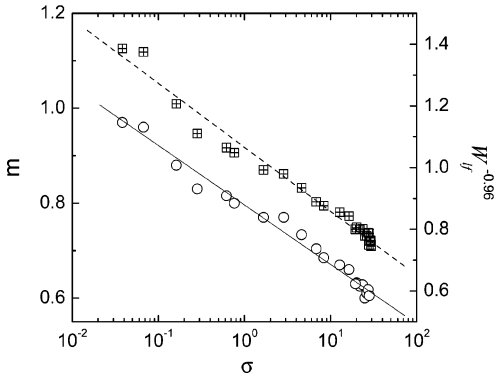

Figure 15. HN shape parameter *m* (○) and low-frequency width W_{lf} (⊞) of the dielectric loss in the reactive system DGEBA−EDA 1:1 (dielectric data from ref 17), plotted vs the variance σ of the cluster size distribution, along with the best fit to a logarithmic decay.

presently available include network and linear polymer-forming formulations, with stoichiometric balance and imbalance of the reagents. Figure 15 reports data for DGEBA cured with a tetrafunctional amine, ethylenediamine (EDA), in the nonstoichiometric ratio of 1:1. Dielectric fit parameters in the course of reaction were taken from ref 17 and used to calculate W_{lf}, from which $m \sim W_{lf}^{-0.96\pm0.02}$. The variance of the molecular size distribution was calculated at any degree of conversion from eq 4 and put into relation with the corresponding values of *m* and W_{lf} (Figure 15). Also in this case we find that *m* and $W_{lf}^{-0.96}$

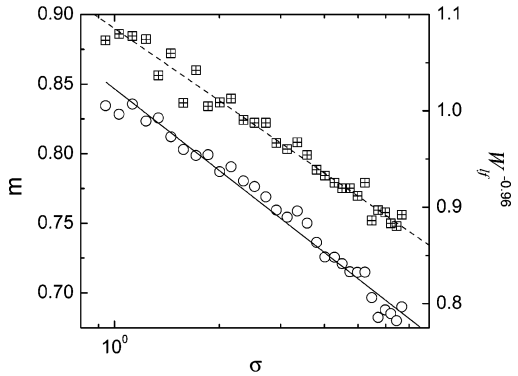

Figure 16. HN shape parameter m (○) and low-frequency width W_{lf} (⊞) of the dielectric loss in the reactive system DGEBA-BAM 1:1 (dielectric data from ref 17), plotted vs the variance σ of the cluster size distribution, along with the best fit to a logarithmic decay.

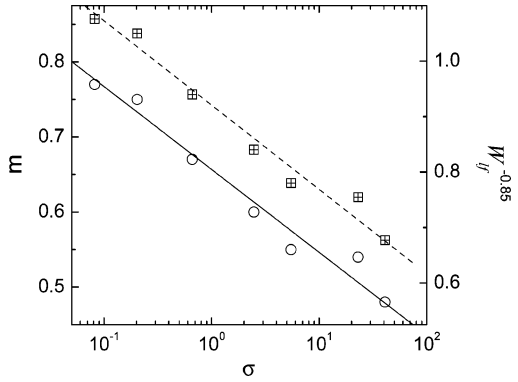

Figure 17. HN shape parameter m (○) and low-frequency width W_{lf} (⊞) of the dielectric loss in the reactive system DGEBA-MDA 2:1 (dielectric data from ref 47), plotted vs the variance σ of the cluster size distribution along with the best fit to a logarithmic decay.

decay logarithmically with σ. As shown in Figure 16, similar relationships fit experimental data for DGEBA cured with the stoichiometric amount of a bifunctional amine, butylamine (BAM), yielding linear chain products. (In both DGEBA−EDA 1:1 and DGEBA−BAM 1:1 systems a dynamic change is documented at $\alpha \sim 0.36$;[17] we therefore restricted attention to higher α values.)

The data in Figure 17 refer to the network-forming formulation consisting of DGEBA and methylenedianiline (MDA) in the stoichiometric ratio of 2:1. They were calculated from the dielectric parameters m and n reported in Table 2 of ref 47 and using eq 4 with $f_e = 2$ and $f_a = 4$. Differently from the DGEBA−DETA mixtures investigated in the present paper and from the DGEBA−EDA and DGEBA−BAM formulations previously examined, the high-frequency dielectric parameter n is reported to vary from 0.50 to 0.33 in the course of reaction. Thus, the measured pairs (m,n) belong to different constant-n lines in Figure 13; nevertheless, we still find m to scale with W_{lf}, with a scaling exponent of -0.85 ± 0.01. Moreover, despite some scattering of the m data, these are in reasonable agreement with a logarithmic decay with σ, over almost 3 decades of variation of σ. Dielectric parameters with a pronounced variation of n, from 0.42 to 0.22, are also reported in ref 47 for the reaction of triglycidyl ether of *p*-aminophenol (TGEPA, $f_e = 3$) with MDA ($f_a = 4$), in the 4:3 molar ratio. Also for this system the dielectric shape evolves in the course of reaction in a manner that m scales with $W_{lf}^{-0.98\pm0.01}$. The few available data of m for TGEPA−MDA 4:3 in the pregel region ($\alpha < 0.4$) are shown as a function of σ in Figure 18. A logarithmic decay is suggested but not established definitively by these data.

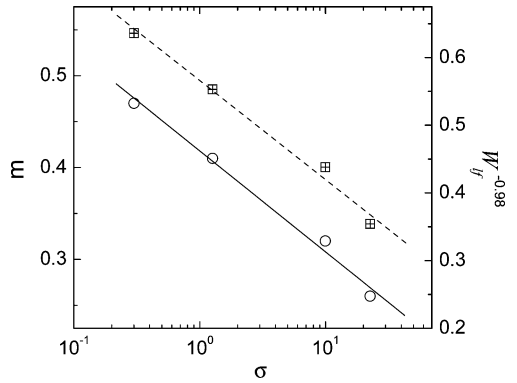

Figure 18. HN shape parameter m (○) and low-frequency width W_{lf} (⊞) of the dielectric loss in the reactive system TGEPA−MDA 4:3 (dielectric data from ref 47) plotted vs the variance σ of the cluster size distribution along with the best fit to a logaritmic decay.

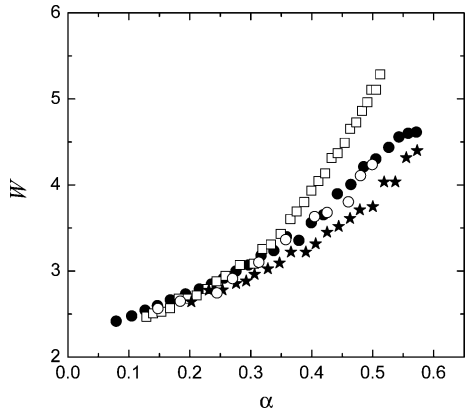

Figure 19. Dependence on conversion, α, of the total width at half-height of $\epsilon''(\omega)$, W, for the reactive mixtures DGEBA−DETA 10:3 (□), DGEBA−DETA 5:2 (●), DGEBA−DETA 5:2.8 (○), and DGEBA−DETA 10:9 (★). Notice that the total width also includes the high-frequency contribution to the broadening of the dielectric loss spectra ($W > W_{lf}$).

A final remark concerns the comparison of the present findings with a previously proposed methodology to correlate dipole dynamics to the kinetics of network formation,[47] involving the analysis of dielectric broadening. The method is based on the observation that a relative change in the width at half-heigth of the loss peak (W) for the stoichiometric formulations of DGEBA−MDA and TGEPA−MDA was in agreement with the extent of polymerization determined by near-infrared spectroscopy. As shown in Figure 19, we rather find in all DGEBA−DETA mixtures a nonlinear dependence on α of the width at half-height of the dielectric loss. These findings are not contradicting those presented in ref 47; rather, we simply conclude that the dielectric width cannot be generally used to monitor the rate of formation of a thermoset network.

E. Concluding Remarks

Unveiling the molecular processes at the basis of the slowdown and broadening of the structural relaxation holds the key to understanding the origin of the dynamical arrest of disordered states of matter. Here we have studied how the evolution of the structural relaxation function is connected to the development of particle clusters in DGEBA−DETA mixtures undergoing step polymerization, in which approaching the glassy state is accompanied by a marked decrease of the low-frequency shape parameter. We find that the slowdown of the dynamics is controlled by the average cluster size, whereas the low-frequency broadening of the relaxation function is associ-

ated with increasing polydispersity and consequently more spatial heterogeneity.

Results reported in this work for the relaxation time confirm the existence of general characteristics of the liquid-to-glass transition induced by polymerization in common to the vitrification process observed in supercooled and overcompressed liquids and in many different systems. Indeed, we find that the increase of the relaxation time in the advanced stage of the molecular slowdown can be successfully explained within an entropy model, similar to what is found in molecular liquids.[17,18,78−81] A recent paper[82] showed that the similarity between polymerization-induced and ordinary glass transition also concerns the early stage of the molecular slowdown, where the nonergodicity factor of DGEBA−DETA mixtures conforms to the cusplike behavior of the mode coupling theory prediction. From the fact that the concept of growing clusters, herein considered in polymer-forming systems, often recurs in connection with the evolution of the dynamic properties of systems without chemical bonding,[2−7,83−86] it is tempting to suggest that further similarity may exist. In this scenario, results presented in this work stimulate experimental and numerical studies to understand how the shape of the structural relaxation function in other classes of systems undergoing glass transition is influenced by the characteristics of the distribution of clusters identified near the transition.

Acknowledgment. R.V. acknowledges funding by Consorzio CRESCI. S.C. acknowledges support from MIUR-FIRB (Projects NANOPACK and RBAU01K2E2) and MIUR-PRIN. We thank F. Sciortino and A. Jurlewicz for very helpful discussions.

References and Notes

(1) Angell, C. A. *Science* **1995**, *267*, 1924.
(2) Kob, W.; et al. *Phys. Rev. Lett.* **1997**, *79*, 2827.
(3) Donati, C.; et al. *Phys. Rev. Lett.* **1998**, *80*, 2338.
(4) Tata, B. V. R.; Mohanty, P. S.; Valsakumar, M. C. *Phys. Rev. Lett.* **2002**, *88*, 018302.
(5) Giovambattista, N.; et al. *Phys. Rev. Lett.* **2003**, *90*, 085506.
(6) Dudowicz, J.; Freed, K. F.; Douglas, J. F. *J. Chem. Phys.* **2006**, *124*, 064901.
(7) Giovambattista, N.; et al. *J. Chem. Phys.* **2005**, *72*, 011202.
(8) Adam, G.; Gibbs, J. H. *J. Chem. Phys.* **1965**, *43*, 139.
(9) Pochan, J. M.; Gruber, R. J.; Pochan, D. F. *J. Polym. Sci., Polym. Phys. Ed.* **1981**, *19*, 143.
(10) Sheppard, N. F., Jr.; Senturia, S. D. *J. Polym. Sci., Part B: Polym. Phys.* **1989**, *27*, 753.
(11) Koike, T.; Tanaka, R. *J. Appl. Polym. Sci.* **1991**, *42*, 1333.
(12) Corezzi, S.; Campani, E.; Rolla, P. A.; Capaccioli, S.; Fioretto, D. *J. Chem. Phys.* **1999**, *111*, 9343.
(13) Corezzi, S.; et al. *J. Chem. Phys.* **2002**, *117*, 2435.
(14) Corezzi, S.; et al. *Philos. Mag. B* **2002**, *82*, 339.
(15) Comez, L.; et al. *Phys. Rev. E* **1999**, *60*, 3086.
(16) Corezzi, S.; Rolla, P. A.; Paluch, M.; Zioło, J.; Fioretto, D. *Phys. Rev. E* **1999**, *60*, 4444.
(17) Corezzi, S.; Fioretto, D.; Casalini, R.; Rolla, P. A. *J. Non-Cryst. Solids* **2002**, *307−310*, 281.
(18) Casalini, R.; et al. *Phys. Rev. E* **2001**, *64*, 41504.
(19) Paluch, M.; Patkowski, A.; Fischer, E. W. *Phys. Rev. Lett.* **2000**, *85*, 2140.
(20) Paluch, M.; Roland, C. M.; Gapinski, J.; Patkowski, A. *J. Chem. Phys.* **2003**, *118*, 3177.
(21) Ferrari, C.; Salvetti, G.; Tombari, E.; Johari, G. P. *Phys. Rev. E* **1996**, *54*, R1058.
(22) Schawe, J. E. K.; Alig, I. *Colloid Polym. Sci.* **2001**, *279*, 1169.
(23) Tombari, E.; Ferrari, C.; Salvetti, G.; Johari, G. P. *J. Phys.: Condens. Matter* **1997**, *9*, 7017.
(24) Wasylyshyn, D. A.; Johari, G. P. *J. Polym. Sci., Part B: Polym. Phys.* **1997**, *35*, 437.
(25) Johari, G. P.; Ferrari, C.; Tombari, E.; Salvetti, G. *J. Chem. Phys.* **1999**, *110*, 11592.
(26) Tombari, E.; Salvetti, G.; Johari, G. P. *J. Chem. Phys.* **2000**, *113*, 6957.
(27) Schawe, J. E. K. *Thermochim. Acta* **2002**, *391*, 279.
(28) Zvetkov, W. L. *Polymer* **2002**, *43*, 1069.
(29) Fournier, J.; Williams, G.; Duch, C.; Aldridge, G. A. *Macromolecules* **1995**, *28*, 2797.
(30) Corezzi, S.; Fioretto, D.; Puglia, D.; Kenny, J. M. *Macromolecules* **2003**, *36*, 5271.
(31) Alig, I.; Lellinger, D.; Nancke, K.; Rizos, A.; Fytas, G. *J. Appl. Polym. Sci.* **1992**, *44*, 829 and references therein.
(32) Younes, M.; Wartewig, S.; Lellinger, D.; Strehmel, B.; Strehmel, V. *Polymer* **1994**, *35*, 5269.
(33) Matsukawa, M.; Okabe, H.; Matsushige, K. *J. Appl. Polym. Sci.* **1993**, *50*, 67.
(34) Winter, H. H. *Prog. Colloid Polym. Sci.* **1987**, *75*, 104.
(35) Golub, M. A.; Lerner, N. R. *J. Appl. Polym. Sci.* **1986**, *32*, 5215.
(36) Fitz, B. D.; Mijović, J. *Macromolecules* **1999**, *32*, 4134.
(37) Mijović J.; Andjelić S.; Winnie, Yee, C. F.; Bellucci, F.; Nicolais, L. *Macromolecules* **1995**, *28*, 2797.
(38) Mijović, J.; Andjelić, S. *Polymer* **1996**, *37*, 1295.
(39) Lachenal, G.; Pierre, A.; Poisson, N. *Micron* **1996**, *27*, 329.
(40) Yamanaka, K.; Inoue, T. *Polymer* **1989**, *30*, 662.
(41) Mangion, M. B. M.; Vanderwal, J. J.; Walton, D.; Johari, G. P. *J. Polym. Sci., Part B: Polym. Phys.* **1991**, *29*, 723 and references therein.
(42) Matsukawa, M.; Yamura, H.; Nakayama, S.; Otani, T. *Ultrasonics* **2000**, *38*, 466.
(43) *Dielectric Spectroscopy of Polymeric Materials; Fundamentals and Applications*; Runt, J. P., Fitzgerald, J. J., Eds.; American Chemical Society: Washington, DC, 1997.
(44) *Dielectric Relaxation Spectroscopy; Fundamentals and Applications*; Kremer, F., Schonhals, A., Eds.; Springer: Berlin, 2000.
(45) Bellucci, F.; Valentino, M.; Monetta, T.; Nicodemo, L.; Kenny, J. M.; Nicolais, L.; Mijiović, J. *J. Polym. Sci., Phys. Ed.* **1994**, *32*, 2519.
(46) Williams, G.; Smith, I. K.; Holmes, P. A.; Varma, S. *J. Phys.: Condens. Matter* **1999**, *11*, A57.
(47) Andjelić, S.; Fitz, B. D.; Mijiović, J. *Macromolecules* **1997**, *30*, 5239.
(48) Cassettari, M.; Salvetti, G.; Tombari, E.; Veronesi, S.; Johari, G. P. *J. Non-Cryst. Solids* **1994**, *172−174*, 554.
(49) Levita, G.; Livi, A.; Rolla, P. A.; Culicchi, C. *J. Polym. Sci., Part B: Polym. Phys.* **1996**, *34*, 2731.
(50) Casalini, R.; Corezzi, S.; Fioretto, D.; Livi, A.; Rolla, P. A. *Chem. Phys. Lett.* **1996**, *258*, 470.
(51) Gallone, G.; Capaccioli, S.; Levita, G.; Rolla, P. A.; Corezzi, S. *Polym. Int.* **2001**, *50*, 545.
(52) Parthun, M. G.; Johari, G. P. *J. Chem. Phys.* **1995**, *103*, 440.
(53) Fitz, B. D.; Andjelić, S.; Mijović, J. *Macromolecules* **1997**, *30*, 5227.
(54) Stockmayer, W. H. *J. Polym. Sci.* **1952**, *9*, 69.
(55) Flory, P. *J. Chem. Rev.* **1946**, *39*, 137.
(56) Corezzi, S.; Fioretto, D.; Kenny, J. M. *Phys. Rev. Lett.* **2005**, *94*, 065702.
(57) Schmidt-Rohr, K.; Spiess, H. W. *Phys. Rev. Lett.* **1991**, *66*, 3020.
(58) Roland, C. M. *Macromolecules* **1994**, *27*, 4242.
(59) Young, R. J.; Lovell, P. A. *Introduction to Polymers*; Chapman and Hall: New York, 1991.
(60) Corezzi, S.; Fioretto, D.; Rolla, P. A. *Nature (London)* **2002**, *420*, 653.
(61) Flory, P. J. *Principles of Polymer Chemistry*; Cornell University Press: Ithaca, NY, 1953.
(62) The secondary relaxation has been described by setting $n_s = 0.4$, as found in similar epoxy−amine systems.[51] Note that for some of the analyzed spectra (with a high degree of overlapping of the relaxations) an independent determination of all the other parameters was not possible. In these cases, some of the parameters were fixed (as indicated in the caption of Figures 4−7) or constrained within a narrow range around the values extrapolated from the near conversion regions.
(63) Beiner, M.; Ngai, K. L. *Macromolecules* **2005**, *38*, 7033.
(64) Mijović, J.; Zhang, H. *Macromolecules* **2003**, *36*, 1279.
(65) Dominguez-Espinosa, G.; Díaz-Calleja, R.; Riande, E.; Gargallo, L.; Radic, D. *J. Chem. Phys.* **2005**, *123*, 114904.
(66) Dominguez-Espinosa, G.; Díaz-Calleja, R.; Riande, E.; Gargallo, L.; Radic, D. *Macromolecules* **2006**, *39*, 3071.
(67) Paluch, M.; Rzoska, S. J.; Habdas, P.; Zioło, J. *J. Phys.: Condens. Matter* **1998**, *10*, 4131 and references therein.
(68) Vogel, H. *Phys. Z.* **1921**, *22*, 645. Tammann, G.; Hesse, W. *Z. Anorg. Allg. Chem.* **1926**, *156*, 245.
(69) Bovelli, S.; Fioretto, D.; Jurlewicz, A. *J. Phys.: Condens. Matter* **2001**, *13*, 373.
(70) This is also the reason why the Fourier transform of the KWW function can be described by a Cole−Davidson function which is characterized by a single high-frequency shape parameter (Lindsey, C. P.; Patterson, G. D. *J. Chem. Phys.* **1980**, *73*, 3348), even if a HN function produces a better interpolation (Alvarez, F.; Alegría, A.; Colmenero, J. *Phys. Rev. B* **1993**, *47*, 125).

(71) Alegría, A.; Macho, E.; Colmenero, J. *Macromolecules* **1991**, *24*, 5196.
(72) Weron, K.; Jurlewicz, A.; Jonscher, A. K. *IEEE Trans. Dielectr. Electr. Insul.* **2001**, *8*, 352.
(73) Jurlewicz, A.; Weron, K. *J. Non-Cryst. Solids* **2002**, *305*, 112.
(74) Jonscher, A. K.; Jurlewicz, A.; Weron, K. *Contemp. Phys.* **2003**, *44*, 329.
(75) Jurlewicz, A. *Appl. Math.* **2003**, *303*, 325.
(76) Schönhals, A.; Schlosser, E. *Colloid Polym. Sci.* **1989**, *267*, 125.
(77) Stauffer, D.; Aharony, A. *Introduction to Percolation Theory*; Taylor & Francis: London, 1992; Chapter 2.
(78) Roland, C. M.; Capaccioli, S.; Lucchesi, M.; Casalini, R. *J. Chem. Phys.* **2004**, *120*, 10640.
(79) Prevosto, D.; Lucchesi, M.; Capaccioli, S.; Casalini, R.; Rolla, P. A. *Phys. Rev. B* **2003**, *67*, 174202.
(80) Casalini, R.; Paluch, M.; Fontanella, J. J.; Roland, C. M. *J. Chem. Phys.* **2002**, *117*, 4901.
(81) Paluch, M.; Casalini, R.; Best, A.; Patkowski, A. *J. Chem. Phys.* **2002**, *117*, 7624.
(82) Corezzi, S.; Comez, L.; Fioretto, D.; Monaco, G.; Verbeni, R. *Phys. Rev. Lett.* **2006**, *96*, 255702.
(83) Sciortino, F.; Mossa, S.; Zaccarelli, E.; Tartaglia, P. *Phys. Rev. Lett.* **2004**, *93*, 055701.
(84) Sciortino, F.; Tartaglia, P.; Zaccarelli, E. *J. Phys. Chem. B* **2005**, *109*, 21942 and references therein.
(85) Zaccarelli, E.; et al. *J. Chem. Phys.* **2006**, *124*, 124908.
(86) Lu, P. J.; Conrad, J. C.; Wyss, H. M.; Schofield, A. B.; Weitz, D. A. *Phys. Rev. Lett.* **2006**, *96*, 028306.

MA0627323